Microstructural Characterization of Micro- and Nanoparticles Formed by Polymer−Surfactant Interactions

G. Nizri,[†] S. Magdassi,[†] J. Schmidt,[‡] Y. Cohen,[‡] and Y. Talmon*[,‡]

Casali Institute of Applied Chemistry, The Hebrew University of Jerusalem, Jerusalem 91904, Israel, and Department of Chemical Engineering, Technion-Israel Institute of Technology, Haifa 32000, Israel

Received December 23, 2003. In Final Form: March 2, 2004

We have studied the nano- and microparticles formed by complexation of PDAC [poly(diallyldimethylammoniumchloride)] and SDS (sodium dodecyl sulfate). The complexation phenomenon was characterized by light scattering and ζ-potential measurements. The nature of the complexes was revealed by direct-imaging cryogenic temperature transmission electron microscopy (cryo-TEM), showing nanometric details of the complexes formed around the point of neutralization. The images also reveal how those aggregates are solubilized by excess surfactant, first into faceted particles with threadlike micelles attached to their surfaces, prior to complete solubilization, then into lacelike aggregates, and finally into spheroidal micelles. The nanostructure of the complexes strongly suggests they are made of a hexagonal liquid crystalline phase. This was further supported by small-angle X-ray scattering (SAXS).

Introduction

The interaction between polymers and surfactants in aqueous solutions has attracted much interest in recent years due to the application of mixed polymer−surfactant systems in various material systems, such as detergents, hair-care products, foams, emulsions, and mineral oil recovery, and in gene-therapy DNA−lipid complexes.

Systems of a neutral polymer with an anionic surfactant, or of a charged polymer with a surfactant of opposite charge, have been extensively studied.[1−8] Most studies have focused on the bulk solution behavior, such as phase diagrams, rheology, light scattering, binding isotherms, and the surface tension of the solutions.[9,10] Most of the investigated systems were composed of nonionic polymers and ionic surfactants, where the surfactant, as a single molecule or as an aggregate, is weakly bound to the polymer chains. In the case of a charged polymer and an oppositely charged surfactant, phase separation usually takes place due to strong electrostatic attraction forces. At certain surfactant concentration range this leads to precipitation of a polymer−surfactant complex. However, it was established that aggregation in such systems could occur at a certain charge ratio without accompanying precipitation.[11] The interactions between an ionic surfactant and an oppositely charged polymer may be characterized by three distinct concentration zones: a clear solution zone, in which the polymer is in excess, a precipitation zone, where the surfactant-to-polymer ratio is close to charge neutralization, and a clear solution resolubilization zone, where excess surfactant solubilizes the complex.

In aqueous solutions without a polymer, surfactants self-aggregate into micelles starting at a well-defined critical micellization concentration (cmc). Similarly, in the presence of a polymer, micelle-like aggregates begin to form at a critical aggregation concentration (cac). Thus cac is an analogue of cmc in solutions of surfactants with added polymeric component. A characteristic feature of this parameter is that it is always lower than the cmc of the corresponding surfactant. Binding of surfactant to the polymer, which may depend on several parameters, such as charge density, surfactant structure, and ionic strength, can lead to the formation of characteristic micro- and nanostructures.

Indeed, cryogenic temperature transmission electron microscopy (cryo-TEM) revealed in a system composed of sodium dodecyl sulfate (SDS) and a quaternary ammonium-substituted hydroxyethylcellulose polymer (JR-400) a variety of microstructures, such as globular particles, vesicles, and disklike and threadlike aggregates.[12]

In the present study we investigate the conditions at which interaction between an anionic surfactant, SDS, and the cationic polyelectrolyte poly(diallyldimethylammoniumchloride), PDAC (Chart 1), lead to formation of nano- and microparticles, and we evaluate the properties of those aggregates.

Experimental Section

Materials. PDAC of molecular weight 100 000−200 000 g/mol, purchased from Aldrich as a 21.8% (w/w) aqueous solution, and

* Corresponding author.
[†] The Hebrew University of Jerusalem.
[‡] Technion-Israel Institute of Technology.

(1) Winnik, F.; Regismond, S. T. A.; Picullel, L.; Lindman, B.; Karlstrom, G.; Zana, R. In *Polymer Surfactant Systems*; Kwak, J. C. T., Ed.; Marcel Dekker: New York, 1998; Vol. 77, pp 267−316, 65−142, and 409−454.
(2) Goddard, E. D.; Ananthapandmanabhan, K. P. In *Interactions of surfactants with polymers and proteins*; CRC Press: Boca Raton, FL, 1993 (2002).
(3) Cabane, B.; Duplessix, R. *J. Colloid Surf.* **1985**, *13*, 19.
(4) Brackman, J. C.; Engberts, J. B. F. N. *J. Colloid Interface Sci.* **1989**, *132*, 250.
(5) Brackman, J. C.; Engberts, J. B. F. N. *Langmuir* **1991**, *7*, 2097−2102.
(6) Goddard, E. D. *Colloids Surf.* **1986**, *19*, 301.
(7) Lindman, B.; Thalberg, K. In *Polymer−Surfactant Interactions*; Goddard, E. D., Ananthapandmanabhan, K. P., Eds.; CRC Press: Boca Raton, FL, 1993; p 203.
(8) Thünemann, A. F. *Prog. Polym. Sci.* **2002**, *27*, 1473−1572.
(9) Staples, E.; Tucker, I.; Penhold, J.; Warren, N.; Thomas, R. K.; Taylor, J. F. *Langmuir* **2002**, *18*, 5147−5153.
(10) Anthony, O.; Marques, C. M.; Richetti, P. *Langmuir* **1998**, *14*, 6086−6095.
(11) Dubin, P. L.; Oteri, R. *J. Colloid Interface Sci.* **1983**, *95*, 453−461.
(12) Goldraich, M.; Schwartz, J. R.; Burns, J. L.; Talmon, Y. *Colloids Surf. A* **1997**, *125*, 231−244.

10.1021/la0364441 CCC: $27.50
Published on Web 04/27/2004

Chart 1

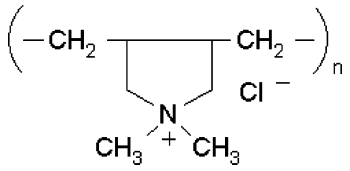

SDS (minimum 98.5%, by gas chromatography) purchased from Sigma, were used without further purification.

Sample Preparation. A constant concentration of PDAC was used in every series of measurements (size, ζ potential, and cryo-TEM observations). An SDS stock solution was prepared by weighing the dry substance and dissolving it in a measured volume of deionized water (0.2 μm filtered). In each experiment series the samples were prepared as follows: 5 mL of SDS solution of the required concentration and 5 mL of PDAC solution (0.2% w/w) were poured simultaneously into a vial and were stirred immediately. Thus, the final PDAC concentration was kept constant, 0.1% w/w (6.8 mM, based on the monomer) in all experiments, while the SDS:PDAC molar ratio was varied. All results were related to the charge ratio, *r*, calculated from the MW of the monomeric unit of the polymer, which has one positive charge, and the SDS molar concentration. After mixing of the solutions, the samples were left in a cuvette for 72 h before measurements were taken at 25 °C.

Size and ζ potential measurements were performed with a ZetaMaster 3000 (Malvern Instruments). Size measurements were performed with a HPPS (high-performance particle sizer, Malvern Instruments). The SDS−PDAC samples, as aqueous dispersions, were placed in a cuvette and measured without dilution. The HPPS instrument is capable of measuring concentrated samples since light is backscattered from the cell to reduce multiple scattering. Therefore, all the particle size data presented here relate to samples without dilution. The calculation of size distribution from light scattering measurements is based on the assumption that the particles are spherical. Because the nanoparticles are not ideal spheres, as shown by cryo-TEM, the size measurements give relative values rather than absolute size. The samples of *r* ratios 0.22 and 0.30, which appeared very clear, were filtered before size measurements by a 0.45 μm filter, since at those concentrations and charge ratios the scattering signal was low, and therefore the measurements are more affected by particles such as dust, compared to the other samples, which were more turbid. The ζ potential was calculated automatically from the measured electrophoretic mobility, by the Henry equation: $U_e = \epsilon\zeta f/6\pi\eta$, where U_e is the electrophoretic mobility, ϵ is the dielectric constant, η is the viscosity, and ζ is the zeta potential. The Smoluchowski factor, $f = 1.5$, was used for the conversion of mobility to ζ potential.[13]

Cryo-TEM specimens were prepared at controlled temperature and relative humidity in a controlled environment vitrification system (CEVS) to avoid water loss and structural changes during specimen preparation.[14] A sample drop was placed on a TEM grid covered by a perforated carbon film. The drop was blotted with a filter paper to form a thin liquid film on the grid (typically 0.25 μm thick), and immediately plunged into liquid ethane at its freezing temperature. Specimens were kept at about −180 °C and observed in a Philips CM 120 transmission electron microscope at an accelerating voltage of 120 kV. We used an Oxford Instruments CT-3500 cryospecimen holder and transfer system. Images were digitally recorded with a Gatan MultiScan 791 cooled CCD camera.

Small-angle X-ray scattering (SAXS) measurements were performed on a small-angle diffractometer (Bruker Nanostar, KFF CU 2 K-90) with Cu Kα radiation, pinhole collimation that gives a beam 100 μm in diameter and a 10 × 10 cm^2 two-dimensional position-sensitive wire detector placed 65 cm behind the examined sample. Solutions were placed in thin-walled glass capillaries sealed with epoxy resin. The dried sample was placed between thin polyimide sheets.

(13) Shaw, D. J. In *Introduction to Colloid and Surface Chemistry*; Butterworth-Heinemann Ltd.: Oxford, U.K., 1991; 4th ed., p 202.

(14) Bellare, J. R.; Davis, H. T.; Scriven, L. E.; Talmon, Y. *J. Electron Microsc. Technol.* **1988**, *10*, 87−111.

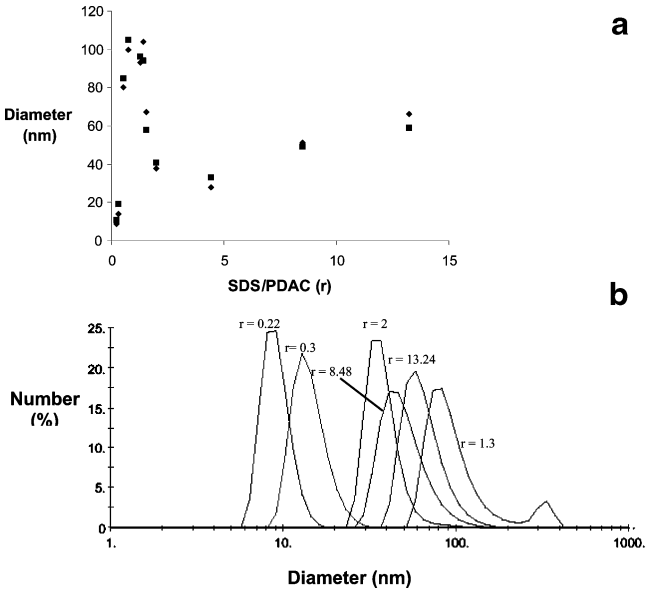

Figure 1. (a) Light scattering results showing average diameter of particles as a function of SDS/PDAC molar ratio. PDAC final concentration in all samples is 6.8×10^{-3} M (based on the monomeric unit) SDS concentration is varied from 1.5×10^{-3} to 0.2 M. Duplicate results are shown for each *r* ratio. (b) Size distribution of SDS−PDAC aggregates at different *r* ratios.

Results and Discussion

Size Measurements. Upon mixing the polymer and the surfactant solutions, some of the systems turn turbid immediately. That turbidity depends on the surfactant-to-polymer molar ratio, expressed as monomeric charge ratio, *r*. Dynamic light scattering size measurements indicate, in general, that particles are formed at all *r* ratios; their size depends on those *r* values. In general, as can be seen from Figure 1a, addition of SDS causes formation of nanoparticles (10−110 nm), until precipitation occurs at about 1:1 charge ratio, or $r = 1$. Above that ratio, particle size decreases again (110 to 40 nm), while at very high *r* values, a slight increase in size is observed, from 40 to 60 nm. At much higher *r* values, e.g., 29.7, the particle size further increases to 330 nm, probably due to aggregation caused by the increase in the ionic strength of the system at that high surfactant concentrations.The size distribution curves of the nanoparticles are presented (Figure 1b) for some of the systems (for clarity of presentation, not all the data are shown in the figure).

ζ Potential. Because the particles are formed by electrostatic interactions, the aggregates were expected to have either positive or negative surface potential, depending on the surfactant-to-polymer charge ratio. Indeed, this is observed by our measurements (Figure 2). It appears that the ζ potential changes according to the *r* ratio: at low *r* (low SDS-to-PDAC molar ratio), the ζ potential is highly positive, +50 to +60 mV. At higher *r* values, the binding of SDS to the positively charged groups of the PDAC molecule leads to nanoparticle ζ potential decrease. At $r \approx 1$, full charge neutralization occurs, and the potential is close to 0. When more SDS is added, it continues to bind to the surfactant−polymer nanoparticles (probably through hydrophobic interactions of the bound SDS chains), hence the aggregates become negatively charged, and at $r = 29.7$ the ζ potential is −45 mV. Some time ago we had found that similar charge reversal occurred in microparticles formed by the interaction of gelatin and a cationic surfactant.[15] The ζ potential remains

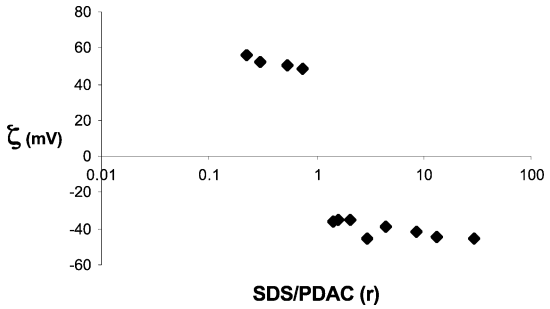

Figure 2. Zeta potential (ζ) of SDS−PDAC particles as function of the SDS/PDAC molar ratio, *r*. PDAC concentration fixed at 6.8×10^{-3} M (based on the monomeric unit); SDS concentration is varied from 1.5×10^{-3} to 0.2 M.

more or less constant over most of two ranges, $r < 1$ and $r > 1$, which may indicate that the binding that causes charge neutralization, followed later by charge reversal, is taking place at a very short range of surfactant/polymer ratios and that at the concentration studied there is no cooperative binding.

The changes in the ζ potential explain the changes in particle size presented above: at low *r* the polymer−surfactant complexes are positively charged and therefore repel each other; thus a dispersion of positively charged nanoparticles is obtained. Upon reaching *r* of 1, that repulsion between the particles vanishes, and therefore large particles precipitate. Further increase of the *r* ratio leads to increased (absolute value) ζ potential, followed by solubilization of the particles, while the negatively charged particles repel each other. Note that the addition of SDS, while increasing the *r* value, increases also the ionic strength of the system. This could lead to the observed increase in particle size, when *r* is increased from 8.48 to 29.7. To prove this possibility, we prepared a system of $r = 2$ and added NaCl to the same ionic strength as SDS at $r = 8.48$. The average particle size in this case was found to be 60 nm, and the ζ potential was −45 mV, very close to the size and ζ potential of the nanoparticles observed at $r = 8.48$. However, the ionic strength is not expected to be affected by the PDAC, because its concentration is very low (6.2 mM) in all samples. Moreover, as a control experiment, we added NaCl to a sample of SDS at a similar concentration to that expected if the polymer is present. In that experiment no formation of nanoparticles was observed, indicating that the formation of nanoparticles does not simply occur due to electrolyte effects. These findings suggest that the surface potential of the nanoparticles is controlled by the *r* value and that the size of the particles can be changed, in the nanometer to micrometer range, by proper selection of the *r* ratio.

Cryo-TEM. This technique provides direct electron micrographs of the polymer−surfactant systems, preserved in their native state, showing nanoscopic details of the inner structure of the aggregates. Here we present a series of cryo-TEM images (Figure 3) that follow the evolution of nanostructures and microstructures with changes in the SDS-to-PDAC molar ratio, *r*. Most images of the aggregates are in agreement with size measurement by dynamic light scattering. However, one has to bear in mind that by cryo-TEM we image single particles, while DLS gives an average size estimation, which is biased toward the larger-size end of the population distribution.

The image at $r = 0.738$ (Figure 3A) is of the only system examined where SDS concentration (5 mM) is below the pure-SDS aqueous solution cmc of 8 mM. It shows a typical aggregate that forms close to the isoelectric point. Those SDS−PDAC complexes exhibit well-ordered domains, with sets of rather long, well-ordered fringes with spacings of about 4 nm. Such fringes may correspond either to an edge view of a lamellar phase or to a side view of a hexagonal phase (normal to the cylinder's long axis). The round objects that seem to be trapped between the fringes (arrowheads) may be cross-section views of the hexagonal phase, making a hexagonal liquid crystalline phase a prime candidate for the structure of those polymer−surfactant complexes. In some aggregates we note that edges of the complexes are faceted (left-hand side of the upper left arrowhead in Figure 3A). The angle of those facets (see also below) is approximately 120° (this number may be somewhat distorted by the position of the edge relative to the electron beam), giving additional support to the suggestion that those complexes are indeed hexagonal liquid crystalline aggregates. The darker "frame" seen in that micrograph is the lacey carbon support film.

At $r = 4.43$ the system is already in the solubilization domain. Indeed, many particles are quite small as seen in the two corresponding panels of Figure 3B,C. The striking features imaged at this composition are relatively short threadlike micelles (arrows in Figure 3B), emerging from many of the aggregate surfaces. Those are probably SDS-rich mixed SDS−PDAC micelles. Similar threadlike micelles, emerging from disks of a lamellar phase, were observed in the process of solubilization of egg-yolk lecithin vesicles by sodium cholate.[16] Many of the smaller aggregates are faceted (arrowheads), with angles about 120°, as also seen above in part of the larger particles imaged at $r = 0.738$. This, again, strongly suggests a hexagonal liquid crystalline phase. One should remember that cryo-TEM images are two-dimensional projections of small three-dimensional objects. In the TEM, due to its very large depth of field, all the details in the relatively thin specimen are projected clearly on the CCD camera detector. Thus, one sees the upper and lower part of the complexes superposed on each other. The projected image is strongly dependent on the relative position of the object to the electron beam. Thus in Figure 3C we notice that fringes are still visible in some aggregates, too. The arrows in Figure 3C point to threadlike structures. The small round dark object in Figure 3B (indicated by F) is an example of frost particles, occasionally seen in the cryo-TEM specimens.

Increasing the *r* to 8.49 leads to further solubilization of the larger aggregates with small, faceted particles (the putative liquid crystalline objects) becoming more abundant. Some of those show threadlike micelles attached to them (Figure 3D). Spheroidal small micelles, probably of free SDS, are seen in the background.

At $r = 13.3$ many of the complexes are solubilized, leaving behind "lacy" objects, probably surfactant-rich (arrows in Figure 3E), and spheroidal micelles in the background. Surprisingly, even at this *r* ratio we can still image particles similar to those seen at lower *r* ratios, with the approximately 120° angle facets, and the "hair" of threadlike micelles attached to them (not shown).

A hexagonal phase, like the apparent one described above, could be made up of SDS cylindrical micelles decorated by PDAC molecules, arranged along the long axis of the cylinders. The quaternary ammonium groups on the polymer chain act in this case as a salt that screens

(15) Vinetsky, Y.; Magdassi, S. *Colloid Polym. Sci.* **1998**, *276*, 395−401.

(16) Walter, A.; Vinson, P. K.; Kaplun, A.; Talmon, Y. *Biophys. J.* **1991**, *60*, 1315−1325.

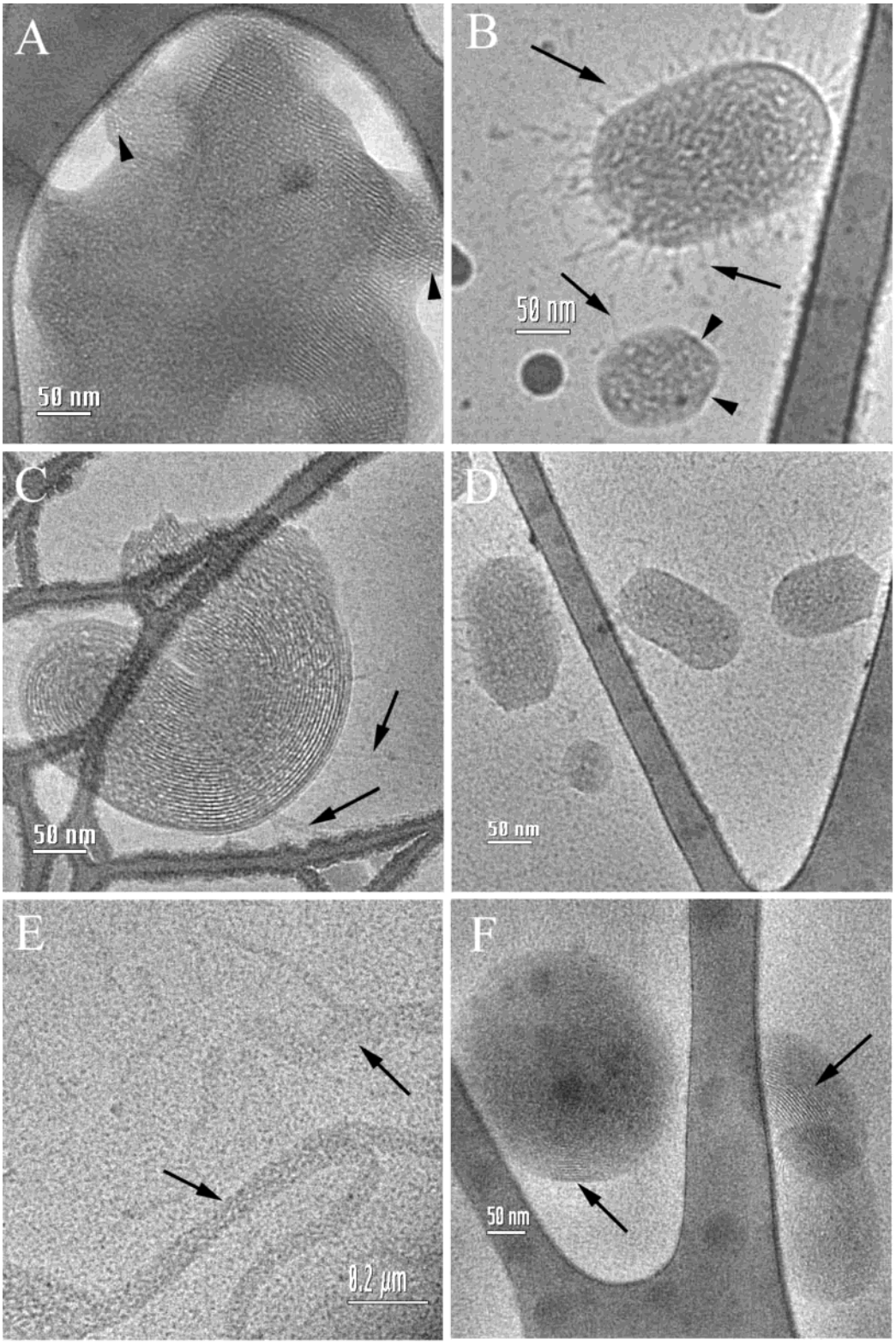

Figure 3. Cryo-TEM images demonstrating the evolution of nanostructure and microstructure with changes in the SDS-to-PDAC molar ratio, *r*, at fixed PDAC concentration of 6.8×10^{-3} M (0.1% w/w). (A) $r = 0.738$; arrowheads point to round objects, possibly cross-section views of the hexagonal phase. (B, C) $r = 4.43$; arrows indicate threadlike micelles; arrowheads point to facets of a liquid crystalline aggregate. (D) $r = 8.49$. (E) $r = 13.3$; arrows indicate partially solubilized complexes. (F) $r = 29.5$; even at this excess of surfactant, some liquid crystalline object, showing fringes (arrows; side views of a hexagonal phase?) are observed.

the electric charges of the negatively charged sulfate groups. The proximity of those groups along the polymer chains makes such alignment quite probable. It is well-known that the addition of salt leads to screening of headgroup charges and induces formation of lower-curvature aggregate. Many examples have been given for such transformation from spheroidal micelles to threadlike ones, e.g., the case of CTABr/NaBr.[17] Thus, the polyelectrolyte acts as a salt that induces threadlike micelle formation and then acts as a "binder" in the hexagonal

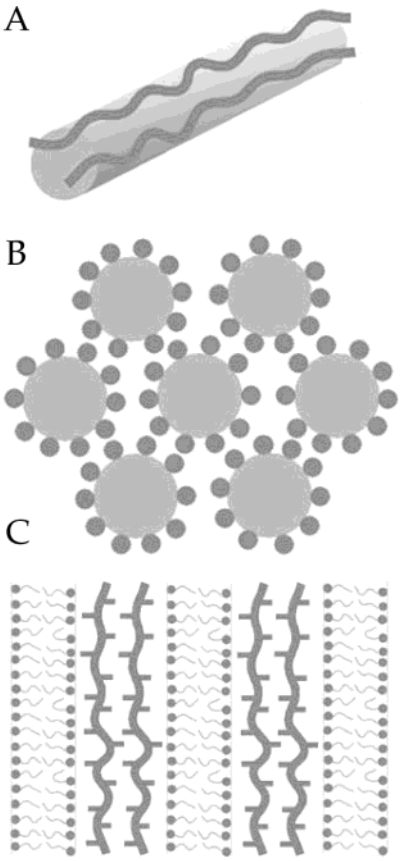

Figure 4. Model for the co-aggregation of SDS and PDAC in a hexagonal phase. (A) Single threadlike micelle shown decorated with two polymer chains. (B) Cross section perpendicular to the long axes of the cylindrical micelles of the hexagonal phase. (C) Cross section along the long axes of the cylindrical micelles.

phase that forms. A similar phenomenon is described by Thünemann,[18] where PDAC apparently leads to the formation of lamellar phases (aggregates of even lower curvature than in our case) when interacting with perfluorinated anionic surfactants. A schematic of the proposed model for the coaggregation of SDS and PDAC in a hexagonal phase is given in Figure 4. Figure 4A shows a single threadlike micelle decorated with two of several polymer chains. Figure 4B is a cross-section (perpendicular to the long axes of the cylindrical micelles) of the hexagonal phase, showing the threadlike micelles (larger disks) decorated by polymer chains (smaller disks). This is the projection one sees in some areas, for example, Figure 3A (see also Figure 5). A cross section along the long axes of the cylindrical micelles is shown in Figure 4C. This view, in projection, leads to the fringes seen in many of the complexes in micrographs of Figure 3.

The suggestion that the aggregates are indeed a hexagonal liquid crystalline phase is further supported by close examination of such a faceted aggregate. Figure 5A shows a cryo-TEM image of an aggregate at $r = 13.3$. This is the unprocessed digital image of the vitrified specimen. Figure 5B shows the fast-Fourier transform (FFT) of the area shown in panel A. The hexagonal symmetry of the structure is quite clear. Figure 5C is the filtered FFT of the transform of panel B, and Figure 5D shows its inverse transform, which is the filtered imaged

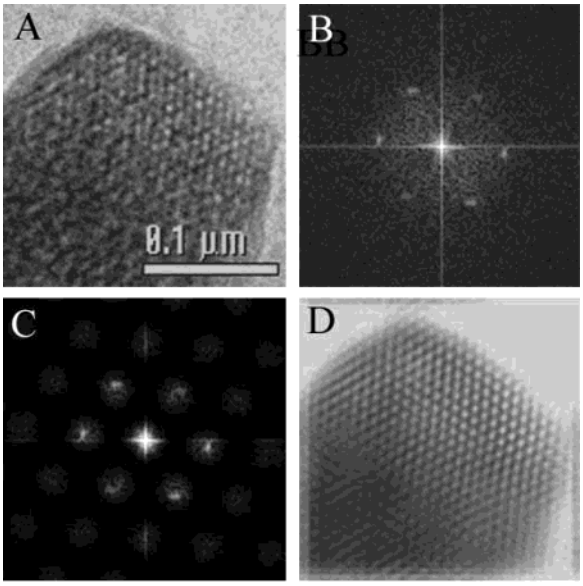

Figure 5. Digital filtering of a cryo-TEM image and complex aggregate at $r = 13.3$. (A) Original, unprocessed digital image. (B) Fast-Fourier transform (FFT) of image A. (C) Filtered FFT of the transform of image B. (D) Inverse transform of image C, i.e., the filtered imaged of the original micrograph.

of the original micrograph. In the filtered image the hexagonal packing is very clear indeed. It should be emphasized that most of those surfactant−polymer complexes show linear fringes as described above. In some cases, nevertheless, small patches of hexagonal array are seen, too. This happens because long slender aggregates tend to align themselves perpendicularly to the thin dimension of the thin cryospecimen, i.e., perpendicularly to the electron beam.

At very high excess of surfactant, e.g., at $r = 29.5$, one would expect complete solubilization and disappearance of all complexes, the expected equilibrium state. Such complete solubilization was indeed observed by us in the study of another SDS−cationic polymer system.[12] However, even at that high r we find in the SDS−PDAC system some complex aggregates in vitrified specimens, which (Figure 3F) still have remnant liquid crystalline structure.

It is interesting to compare the results of the present study with that of our previous work on aqueous dispersions of SDS with the cationic polyelectrolyte JR-400, a quaternary ammonium-substituted hydroxyethylcellulose.[12] While a variety of structures were observed in the latter system, including threadlike micelles, vesicles, and "flocs", no large organized aggregates were imaged. The main difference between the two cases is that the quaternary ammonium group is tightly connected to the backbone of the PDAC polymer chain and is found in much higher frequency along it, as compared to JR-400, where the cations are located at the end of a rather long, flexible side chain and are sparsely positioned along the cellulose chain. Obviously, the structure of PDAC promotes the formation of ordered complexes, as described above, but that of JR-400 does not.

Another useful comparison is between the present work and the system of PDAC with mixture of SDS and Triton X-100 (TX100) studied extensively by Dubin and coworkers,[19−21] with emphasis on the effect of changing the anionic-to-nonionic surfactant concentration ratio. Inter-

(17) Imae, T.; Kamiya, R.; Ikeda, S. *J. Colloid Interface Sci.* **1985**, *108*, 215−225.
(18) Thünemann, A. F. *Polym. Int.* **2000**, *49*, 636−644.
(19) Swanson-Vethamuthu, M.; Dubin, P. L.; Almgren, M.; Li, Y. *J. Colloid Interface Sci.* **1997**, *186*, 424−419.
(20) Wang., Y.; Kimura, K.; Huang, Q.; Dubin, P.; Jaeger, W. *Macromolecules* **1999**, *32*, 7128−7134.

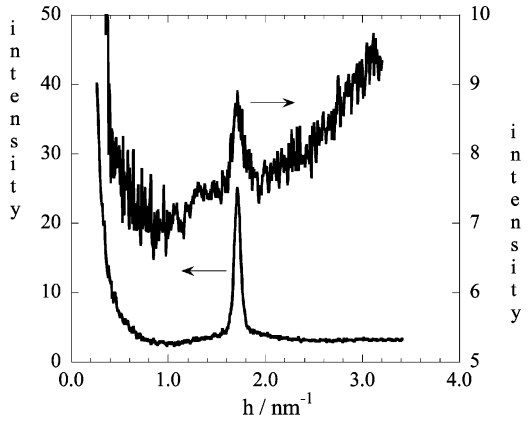

Figure 6. SAXS patterns from SDS−PDAC complex dispersion from 0.1% PDAC solution at $r = 0.9$ (top) and $r = 13.3$ (bottom).

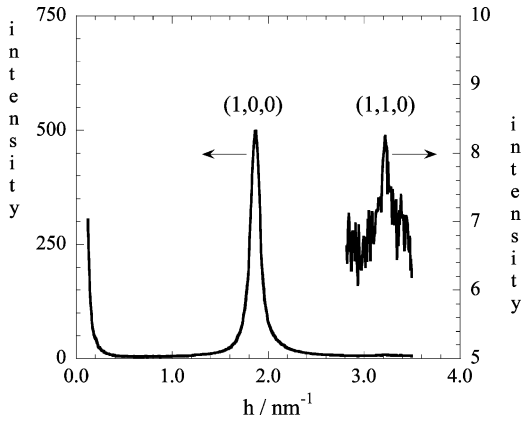

Figure 7. SAXS patterns from SDS−PDAC complex dispersion after drying. The initial dispersion contained 0.1% PDAC at $r = 1$.

estingly, many of the structures observed in our study had not been seen by cryo-TEM performed on the SDS/AOT system.[19] The lesser degree of order may be attributed to the dilution of the negative charge by the nonionic surfactant, leading to weaker binding between surfactant and polymer.

A hexagonal structure of the SDS−PDAC complex was identified by Khokhlov and co-workers in PDAC gels swollen with SDS in water and aqueous salt solutions up to 1 M.[22] Our results of SAXS measurements on the present systems are shown in Figures 6 and 7, where the scattered intensity after circular averaging is plotted as a function of the scattering vector $h = (4\pi/\lambda) \sin \theta$, where λ is X-ray wavelength and θ is half the scattering angle. The SAXS pattern from the dispersion at SDS:PDAC ratio $r = 0.9$, shown in Figure 6 (top curve), exhibits only a single weak reflection at a scattering vector of 1.71 nm^{-1} (Bragg spacing of 3.67 nm). Other dispersions also exhibited weak peaks at a similar spacing. The low intensity of the reflection is due to the low concentration of the complex in the dispersion, yet it clearly shows that even in these dilute dispersions the complex exists in an ordered state. After precipitation of the polymer−surfactant complex by centrifugation, a stronger reflection at the same spacing is exhibited in the SAXS patterns, due to the higher concentration of the denser phase, as shown for the precipitate from the $r = 13.3$ dispersion in Figure 6. The invariance of the peak position indicates that the packing of the structural units is the same in dispersion and after precipitation and does not depend significantly on the SDS:PDAC ratio.

After drying, the condensed phase exhibits a sharp reflection at $h = 1.87$ nm^{-1} (spacing of 3.36 nm), as shown in Figure 7 for a dried sample from a $r = 1.0$ dispersion. A very weak secondary reflection is observed at $h = 3.22$ nm^{-1} (spacing of 1.95 nm), with a maximum intensity about 2 orders of magnitude smaller than the first peak. The ratio of the peak positions is close to $3^{1/2}$, characteristic of a hexagonal lattice. This supports the model of hexagonal packing of polymer-decorated threadlike SDS micelles, shown in Figure 4, based on the TEM images. The absence of second-order peaks in the SAXS patterns from the dispersion and precipitate may be due to the small size of the ordered domains (50−100 nm). Furthermore, there may be a form-factor minimum in the vicinity of the second peak. The structural model presented for the SDS−PDAC complex also suggests a rather tight packing of the threadlike SDS micelles and the polymer in the condensed ordered state. The SAXS measurements can be used to evaluate the amount of water in this condensed state, by comparing the peak positions in the wet (dispersed or precipitate) and dried states. If a hexagonal structure is assumed, loss of water by drying can result in shrinking of the unit cell in two dimensions perpendicular to the cylinder axis. Thus, the water content in the ordered complex domain can be estimated by $[1 - (h_{wet}/h_{dry})^2]$, where h_{dry} (1.87 nm^{-1}) and h_{wet} (1.71 nm^{-1}) are the scattering vectors at the first peaks of the dry and wet states, respectively. This yields an estimated water content of about 16% (v/v), thus verifying that the SDS−PDAC complex is indeed a condensed ordered state.

In conclusion, the formation of SDS−PDAC micro- and nanoparticles have been demonstrated. The ratio between the two components seems to be the main factor in particles size control (according to the change in ζ potential), and cryo-TEM images reveal that the nanoparticles have an ordered inner structure. The cryo-TEM images show quite clearly the 6-fold symmetry in some views of the particles and long fringes in others. Both have a characteristic size of about 4 nm. This direct evidence together with 120° faceting of many of the complex nanoparticle, and the SAXS data, strongly suggest that they consist of a hexagonal liquid crystalline phase.

LA0364441

(21) Wang, Y.; Kimura, K.; Dubin, P.; Jaeger, W. *Macromolecules* **2000**, *33*, 3324−3331.

(22) Mironov, A. V.; Starodoubtsev, S. G.; Khokhlov, A. R.; Dembo, A. T.; Dembo, K. A. *J. Phys. Chem. B* **2001**, *105*, 5612−5617.